Journal of Engineering Science and Technology
Vol. 13, No. 12 (2018) 4078 - 4093

A MODIFIED NON-DOMINATED SORTING GENETIC ALGORITHM FOR MULTI-OBJECTIVE OPTIMIZATION OF MACHINING PROCESS

FARSHID JAFARIAN

Faculty of Engineering, Mahallat Institute of Higher Education, Mahallat, Iran
Email: farshid.jafarian@ymail.com

Abstract

Worn tool geometry when reaches a critical state, has a significant effect on machined surface quality. Identification of the optimal tool life so that the surface quality is kept at a desirable level is an essential task especially in machining of hard materials. Unfortunately, this approach has not been developed enough in literature. In this paper, an experimental study and intelligent methods were used to identify the optimal tool life and surface roughness in turning process of the Inconel 718 alloy. At first, the effect of the machining time at the different cutting parameters (including depth of cut, feed rate and cutting speed) was extensively investigated on the surface roughness using the Artificial Neural Network (ANN) model trained by the optimization algorithm. Then, the modified Non-Dominated Sorting Genetic Algorithm (NSGA-II) was developed to simultaneous optimization of tool life and surface roughness. For this purpose, a new approach was implemented and the machining time was taken into account as both input and output parameter during the optimization. Finally, the results of optimization were classified and the optimal states of the tool life and surface roughness were found. The results indicate that implemented strategy in this paper provides an efficient approach to determine the desirable criterion for tool life estimation in machining processes.

Keywords: Intelligent systems, Surface roughness, Tool life, Turning of inconel 718.

1. Introduction

Inconel 718 superalloy as one of the difficult-to-cut materials is widely used in the aerospace industry and rotary parts of the gas turbine engines. Superior properties of Inconel 718 such as wear resistance, high strength, high melting temperature and maintaining strength and hardness at high temperature are significant reasons for poor machinability of this alloy [1, 2]. It has been shown that tool wear is very evident in machining of Inconel 718 [3]. Apart from tool cost, rapid tool wear leads to stop of the process to change tool and, consequently, decreasing the productivity. Furthermore, tool wear directly affects the surface quality in terms of surface finish and surface alteration. In fact, the surface quality is significantly reduced when tool wear reaches a critical value. Rough machined surface increases the possibility of generation and propagation of the crack in the machined workpiece [4]. The surface roughness of a machined workpiece is one of the most well-known indications of surface finish and plays a critical role in component life and service quality.

(*Ra*) is the most common parameters of surface roughness that is suitable for quality control of manufacturing processes. It is the arithmetic average value of filtered roughness profile determined from deviations about the centre line within the evaluation length. [5]. In addition, the quality of a machined surface in the finishing process where the depth of cut is not too much is mainly affected by tool nose wear. Therefore, it is very important to control the surface roughness and taking into account the effect of tool nose wear during the finishing operation. According to the mentioned descriptions, the main of this study is to find the optimal tool life in finish turning process of Inconel 718 (45 HRC), while the surface roughness is found at the desirable state. According to Khidhir and Mohamed [6], the effect of tool nose wear and cutting speed was studied on surface roughness. They observed the surface roughness was reduced when cutting speed changed from 150 to 250 m/min. Jianxin et al. [7] investigated the failure mechanism of different chemical combinations of ceramic tools. It was found that abrasive wear was dominant for flank wear and also crater wear was occurred using adhesion and diffusion mechanism for all of cutting tools. Darwish [8] studied the effect of cutting parameters and tool material on the surface roughness. Compared with Cubic Boron Nitride (CBN) inserts, the lower surface roughness was reported when ceramic inserts were used. Thakur et al. [9] used tungsten carbide tools to investigate the effect of machining time on cutting forces and flank wear. The results indicated that both tool wear and cutting forces are significantly increased when the machining time increases more than 150 seconds.

Altin et al. [10] investigated the effect of cutting speed on flank wear for different grades of the ceramic tool. It was shown that increasing the cutting speed (more than 250 m/min) leads to the rapid tool wear for all of the cutting tools. As commented by Ezugwu et al. [11], the effect of various coolant supply pressures was investigated under finishing conditions. The tool life is improved by using the pressure up to 15 MPa and it becomes worse at the pressure of 20.3 MPa. Kaynak [12] compared the tool life and surface roughness under dry, MQL (Minimum Quantity Lubricant) and cryogenic conditions in machining with carbide inserts. Higher flank wear was observed in dry conditions especially when machining time increased more than 150 seconds. Also, the lower surface roughness and better surface topography were reported in cryogenic machining.

It should be underlined that it is very difficult and time-consuming to find the optimal machining parameters only by using experimental tests. In fact, number of

the required testing conditions will be too high when the aim is to completely investigate the effect of some input parameters on machining output(s). To solve this problem, the analytical methods and intelligent systems have been used in the scientific community to provide predictive and optimizing models for machining processes [13]. These techniques have been also employed for machining of Inconel 718 alloy. Based on studies by Ezugwu et al. [14] in this regard, the Artificial Neural Network (ANN) model was employed to investigate the effect of machining parameters on surface roughness and tool wear in high speed turning process, although no optimal condition was determined. Homami et al. [15] used intelligent systems based on the ANN model and single optimization algorithm to optimize surface roughness and flank wear at the different cutting speed, feed rate, tool nose radius and approach angle. Jafarian et al. [16] implemented the GONNS (Genetically Optimized Neural Network System) technique to optimize tensile residual stress in finish turning process, while the surface roughness was kept at the desirable ranges. As explained by Pawade and Joshi [17], the surface roughness and cutting forces were simultaneously optimized using Taguchi Grey Relational Analysis (TGRA) in high speed turning process.

It should be noted that tool wear measurement cannot be used as a practical method for customers and engineers since it is not economical to stop the process and measure the tool wear. To overcome this problem, tool wear can be indirectly taken into account by means of tool life (machining time) criterion. Therefore, it is very important to determine the optimal tool life and cutting parameters so that the output(s) of the process is found to be satisfactory. As explained at the above paragraphs, this approach has been never conducted for machining of Inconel 718 superalloy. Therefore, in this study, an intelligent method based on the ANN model, Multi Objective Optimization (MOO) techniques were employed to follow this aim. Based on this, a novel approach was implemented and machining time was defined as both input and output parameter. At first, the effect of input parameters including machining time, depth of cut, feed rate and cutting speed was evaluated on the surface roughness by using the ANN model. Then, the modified Non-dominated Sorted Genetic Algorithm (NSGA) was developed for simultaneous optimization of the surface roughness and tool life during the turning of Inconel 718 alloy.

2. Intelligent Systems in Manufacturing Engineering

Intelligent systems including predictive and optimization models have been used as a beneficial tool in manufacturing processes such as machining processes. Using the predictive models, it is possible to widely investigate the effect of input parameters on output(s) of the process [18]. In addition, the optimization algorithms such as Genetic Algorithm (GA) have been utilized to find optimal conditions at the machining processes [19]. These algorithms can be used for single or multi-objective optimization problems. In the following, more detailed information is provided about predictive and optimization models.

2.1. Artificial neural network (ANN)

Artificial Neural Networks (ANNs) as one of the most well-known predictive models are able to estimate output(s) of the machining processes for the corresponding input parameters. Each neural network includes several neurons organized into the network layers (input, output and hidden layers). Neurons of the

various layers are connected together by using the weighted connection links. Also, an independent weight (bias) can be added to each neuron. Hyperparameters of a neural network including the number of hidden layers, number of neurons and the type of transfer functions are selected to make different topology [20]. Figure 1 shows an example of a multilayer perception neural network with two hidden layers employed in this study.

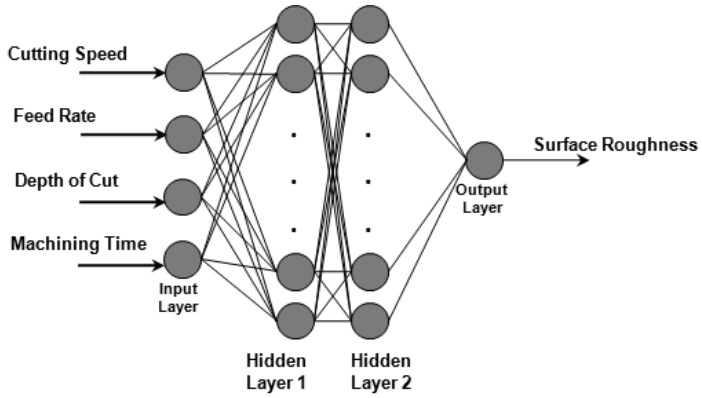

Fig. 1. A multilayer perception neural network.

Training the ANN by optimization algorithm

The process of adjusting weights and biases of a neural network is called network training. It should be underlined that topology and method of training the neural network play a significant role in the accuracy of the predictive model. Therefore, these parameters should be correctly selected for modelling the machining processes. Recently it has been shown that training the ANNs using the evolutionary algorithms (such as GA) is more efficient than other conventional training methods [20]. In this method, a multilayer perception neural network is taken into account as initial neural network topology and weights and biases of the neural network are defined as optimization variables of GA. Then, the MSE (Mean Square Error) between the predicted output and the actual outputs is defined as an objective function of the optimization algorithm. As a result, in each generation weights and biases of the neural network is updated and the MSE of the training data is continuously decreased. More information about this method of training is provided at the author's previous works [16, 20, 21]. For example, a simple ANN topology including 2 and 4 neurons respectively in the input layer and the hidden layer is created to train with an optimization algorithm. The number of optimization variables (N) is extracted from Eq. (1):

$$N = F \times N_h + B_h + N_h \times N_o + B_o \quad (1)$$

where F, N_h, B_h, N_o, B_o are the number of inputs, neurons of the hidden layer, hidden layer biases, output layer neurons and output layer biases, respectively. When the Logsig transfer function is selected, the structure of the neural network can be obtained using Eqs. (2) to (5):

$$S_1 = [W_1] \times [I] + b_1 \quad (2)$$
$$S_2 = Logsig(S_1) \quad (3)$$

$$Z_1 = [W_2] \times S_2 + b_2 \quad (4)$$

$$Z_2 = Logsig(Z_1) \quad (5)$$

where, I and Z_2 are respectively input matrix and the output value of the network. In addition, (p_1, p_2 ... p_{17}) are selected to be optimization variables so that W_1= (p_1 to p_8), b_1= (P_9 to P_{12}), W_2= (p_{13} to p_{16}) and b_2= (p_{17}) are respectively matrixes for weights between input and hidden layer, hidden layer biases, weights between hidden and output layer and output layer bias. The structure of the *ANN* that describes the example is shown in Fig. 2.

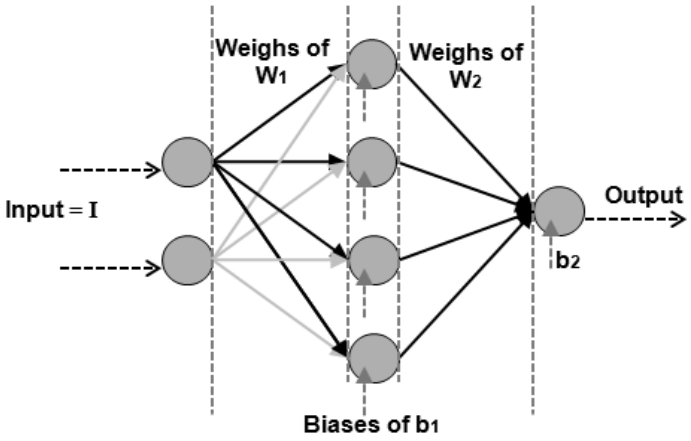

Fig. 2. Structure of ANN for training by GA.

2.2. Multi-objective optimization (MOO)

Many real-life problems are not limited to optimization of one objective and two or more conflicting objectives are required to be optimized at the same time. Therefore, Multi-Objective Optimization (MOO) can be defined as the process of simultaneously optimizing two or more conflicting objectives and it can be found in many fields wherever optimal decisions need to be taken in the presence of trade-offs between two or more conflicting objectives [22]. In multi-objective optimization problems, there are two spaces: decision and objective spaces. As regards the first, decision space involves input variables of problems, while the second's space involves the output value of the problem. Since output variables are related to the particular input values, the main goal of optimization problems is to find the optimal input variables for optimizing the corresponding objective value. In this regard, $x=\{x_1,\ldots, x_n\}$ is n-dimensional vector of input variables in the decision space X and $F(x)=z=\{z_1(x),\ldots, zm(x)\}$ is objective functions of optimization in the objective space Z. Each n-dimensional point in the decision space is mapped into an m-dimensional point in the objective space [23]. Figure 3 illustrates the simple mapping between the decision and objective space in MOO algorithm.

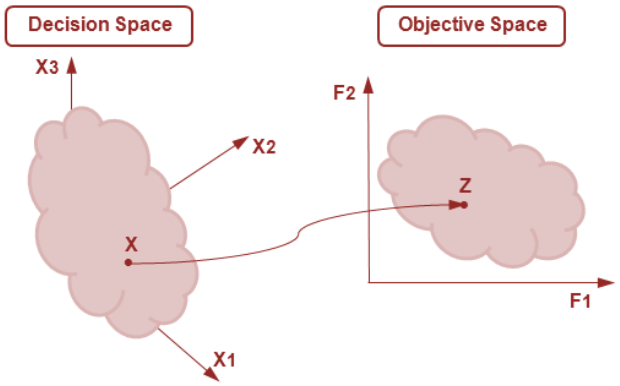

Fig. 3. Simple mapping between decision and objective space in MOO.

2.2.1. Fitness evaluation in MOO

Fitness evaluation in MOO is different from single objective optimization and there are a set of the optimal solution, which dominates other solutions in the decision space. For example, in minimization problems, a feasible solution X is said to dominate other feasible solution y, if and only if, $zi(x) \leq zi(y)$ for $i = 1, \ldots, m$ and $zj(x) < zj(y)$ for at least one objective function j. In this condition, all of the non-dominated solutions in X space is said Pareto optimal and the corresponding objective function values in Z space is called Pareto front [23]. It should be noted that all of the solution set in the Pareto front is not absolutely better than each other, while each solution is better than other solutions at least in one objective.

2.2.2. Non-dominated sorting genetic algorithm (NSGA-II)

At supersonic speeds, the base drag of the body, caused by a large negative pressure, results in a substantial increase in the body drag. The base drag coefficient of the body is related to the base pressure coefficient as follows [4]. NSGA-II (Non-dominated Sorting GA-II) is one of the most popular evolutionary algorithms for solving multi-objective optimization problems. It is an extension of the simple Genetic Algorithm (GA) to solve multi-objective problems [23, 24]. Figure 4 illustrates the main procedure of the basic NSGA-II.

This algorithm starts with a random population of the input variables (P_t). Then the population Qt is created from the parent population Pt by means of the usual genetic operators such as mutation and crossover. After that, the entire population ($Qt + P_t$) is evaluated by using the objective functions, all of them are ranked based on the non-dominated procedure (definition of the MOO) and then sorted according to the ascending order of dominance. Finally, the individuals of the best Pareto front(s) stored on top of the list are directly transferred to the next step (parent population P_{t+1}). This procedure is continued until entire individuals of a particular Pareto front cannot be accommodated fully in the parent population P_{t+1} [23]. Therefore, the crowded comparison operator called crowding distance is employed to select the required individuals and to complete the population P_{t+1}. The crowding distance operation is explained more in the next subsection. At the end, the population P_{t+1} are used instead of the population P_t at the next generation of

NSGA-II and the optimal Pareto front is found after a particular generation. For more information on NSGA-II refer to [23, 25].

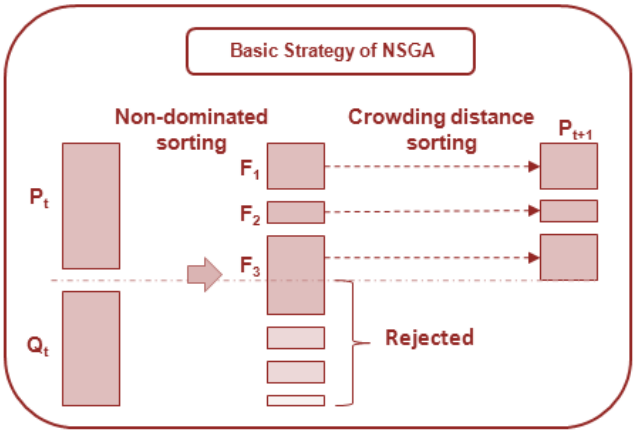

Fig. 4. Basics procedure of the NSGA-II.

2.2.3. Crowding distance operation

Crowding Distance (CD) is a measure to estimate the density of solutions, which surrounds each point in the particular Pareto front. At first, all of the solutions in a particular Pareto front are sort based on the ascending order of the first objective and then the crowding calculations are implement for each solution (cd_1). This procedure (sorting) is repeated for the rest of the objective function(s) and crowding calculations are implemented for each solution (cd_2, cd_3....). Finally, the average of these calculations is identified as a crowding distance criterion for each solution [25]. In fact, diversity of the solutions at the optimal Pareto front is improved using the crowding distance operator, since the individuals with further distance than others are selected for the next generation. Figure 5 shows a schematic view for the determination of crowding distance for each individual (solution member of i). The calculations of the crowding distance operator are also illustrated using Eqs. (6) and (7):

$$\mathrm{cd_k}\left(\mathrm{x_{(i,k)}}\right) = \frac{\mathrm{f_k}\left(\mathrm{x_{(i+1,k)}}\right) - \mathrm{f_k}\left(\mathrm{x_{(i-1,k)}}\right)}{\mathrm{f_k^{max}} - \mathrm{f_k^{min}}} \tag{6}$$

$$\mathrm{cd}\,(\mathrm{x}) = \sum_{\mathrm{k}} \mathrm{cd_k}\,(\mathrm{x}) \tag{7}$$

where k is number of the objective functions, f_k is a kth solution in the objective space, $x_{(i,k)}$ is ith solution in the decision space. In addition, f_k^{max} and f_k^{min} are the maximum and minimum solution of the objective function k, respectively. $cd\,(x)$ is the crowding distance criterion for the solution x.

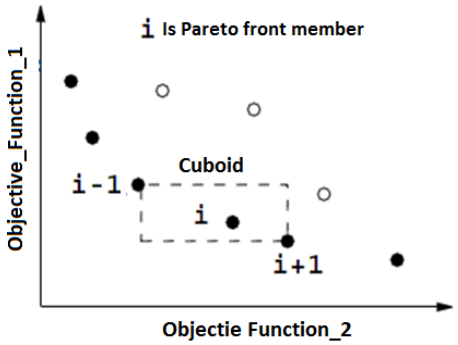

Fig. 5. Determination of crowding distance for each individual.

3. Experimental procedure

The machining tests were conducted on a rigid Machining lathe using cemented carbide tools (VBMT150608). The inserts were mounted on a Sandvik tool-holder (SVJBL1616K16-S). The Inconel 718 samples were solution annealed at 950 °C and then age hardened at 720 °C to the nominal bulk hardness of (47) HRC. The chemical composition of Inconel 718 alloy includes 53.59% Ni, 17.93% Cr, 19.04% Fe, 5.07% Nb, 2.72% Mo, 1.87% Ti, 0.45% Al and 0.05% Si.

In this study, the effect of cutting speed (*Vc*), feed rate (*af*), depth of cut (*ap*) and machining time was evaluated on the surface roughness. The machining tests were carried out under coolant conditions (wet machining) to obtain better surface quality. All of the machining parameters were taken into account in 4 levels as shown in Table 1. The CNC machine used for turning process an example of a worn tool is shown in Fig. 6.

Table 1. Levels of machining parameters for experimental tests.

Machining parameters	Level 1	Level 2	Level 3	Level 4
Cutting speed (*Vc*) m/min	75	100	125	150
Feed rate (*af*) mm/rev	0.02	0.04	0.06	0.08
Depth of cut (*ap*) mm	0.15	0.30	0.45	0.60
Machining time sec	60	120	180	240

(a) CNC machine in wet condition.

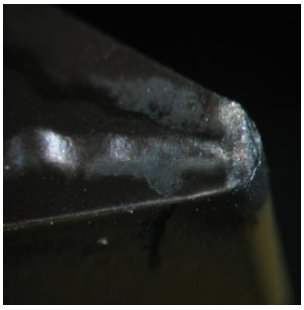

(b) Example of a worn tool.

Fig. 6. Experimental setup for machining process.

The testing conditions were selected based on the design of the experiment. This method uses a desired subset from whole testing conditions to reduce the number of the required experiments. In this study, the testing conditions were selected based on the L_{32} orthogonal array in the Taguchi method. After the machining tests, the surface roughness of the samples was measured and the average of tree measurement was reported as the surface roughness (Ra) value for each test. The experimental results of the surface roughness with corresponding input parameters are presented in Table 2. In the rest of the paper, the experimental results were introduced to the intelligent systems to estimate and optimize the process.

Table 2. Experimental results of the machining tests.

Test number	Depth of cut (mm)	Cutting speed (m/min)	Feed rate (mm/rev)	Machining time (sec)	Surface roughness (μm)
1	0.20	75	0.02	60	**0.2**
2	0.20	100	0.04	120	**0.9**
3	0.20	125	0.06	180	**2.2**
4	0.20	150	0.08	240	**2.3**
5	0.35	75	0.02	120	**1.1**
6	0.35	100	0.04	60	**1.65**
7	0.35	125	0.06	240	**1.10**
8	0.35	150	0.08	180	**1.35**
9	0.50	75	0.04	180	**1.75**
10	0.50	100	0.02	240	**0.60**
11	0.50	125	0.08	60	**0.70**
12	0.50	150	0.06	120	**1.35**
13	0.65	75	0.04	240	**0.38**
14	0.65	100	0.02	180	**1.45**
15	0.65	125	0.08	120	**0.96**
16	0.65	150	0.06	60	**1.35**
17	0.20	75	0.08	60	**0.65**
18	0.20	100	0.06	120	**0.35**
19	0.20	125	0.04	180	**1.15**
20	0.20	150	0.02	240	**0.85**
21	0.35	75	0.08	120	**3.40**
22	0.35	100	0.06	60	**1.35**
23	0.35	125	0.04	240	**1.70**
24	0.35	150	0.02	180	**1.10**
25	0.50	75	0.06	180	**1.35**
26	0.50	100	0.08	240	**0.44**
27	0.50	125	0.02	60	**0.30**
28	0.50	150	0.04	120	**2.10**
29	0.65	75	0.06	240	**0.39**
30	0.65	100	0.08	180	**0.82**
31	0.65	125	0.02	120	**1.35**
32	0.65	150	0.04	60	**1.90**

4. Results and Discussion

In this study, the effect of the tool wear and machining parameters was investigated on the surface roughness at the turning process of Inconel 718 alloy. To do this, the experimental results of the Table 2 were applied to the intelligent systems including ANN and MOO. At the first section, the machining time was

taken into account as an input parameter to train the neural network using GA. Then, the ANN model was used to investigate the effect of the cutting speed, feed rate and depth of cut on the surface roughness at the different machining time. At the second's section, the machining time was introduced as an output of the process to the NSGA-II to simultaneously optimize the surface roughness and tool life in machining of Inconel 718.

4.1. Results of the ANN model

At first, the most suitable network topology was identified using the leave one out cross validation method. More information on this method is given in [21]. Finally, the network with two hidden layers (5 and 4 neurons in first and seconds are hidden layer) and transfer functions of Tansig, Logsig and Tansig for the first hidden layer, seconds hidden layer and output layer was selected, respectively. After the identification of the suitable structure, a number of 27 data (in Table 2) was used to train and rest of the data was used to test the neural network. The neural network was trained using the GA. The input and output data were normalized between 0 and 1 and also MSE of the training data was defined as the *GA* objective function to increase training performance. The early stopping strategy was used to avoid over learning (overfitting) of the network [24]. Based on this, the network was trained at the different iterations and the most suitable iteration was selected for training the network. Finally, the average error of training and testing data was reported at 5.5% and 6.7%, respectively. The comparison between experimental and predicted results for both training and testing data is shown in Fig. 7. As can be seen, the testing and training error is approximately the same and it means the network has been trained adequately.

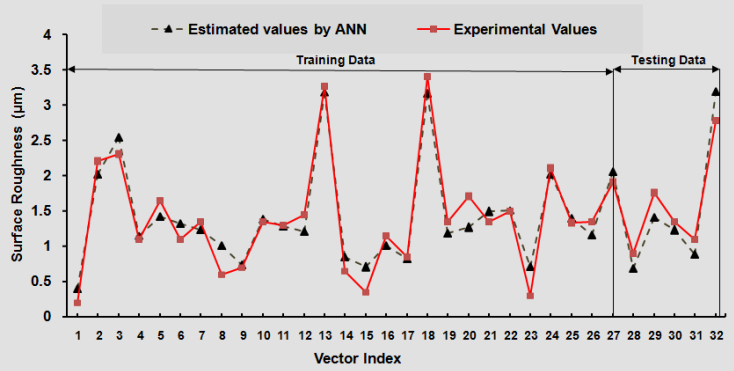

Fig. 7. Comparison between estimated and experimental values.

4.2. Multi-objective optimization of the process

4.2.1. Implementation of the modified NSGA-II on a benchmark function

In this section, the process was simultaneously optimized using Non-dominated Sorting Genetic Algorithm (NSGA-II). It has been shown that the diversity of the Pareto front in NSGA-II is improved by implementing the elitism strategy [25]. Thus, in the present study, the NSGA-II was written in MATLAB software and the elitism strategy was added to the algorithm. In this method, the population of the

other Pareto fronts (dominated solutions) can be transferred to the next generation by using the Eq. (8) [25]:

$$N_j = N\left(\frac{1-r}{1-r^K}\right) r^{1-j} \tag{8}$$

where Nj is a number of allowable population that is selected from the j^{th} non-dominated set, N is the population size, K is number of the Pareto fronts and $0 < r < 1$ is the reduction rate. This algorithm was examined on the benchmark function of ZDT6 (test function). Finally, the obtained Pareto front was the same as the Pareto front reported in other modified NSGA-II [25]. The test function of the ZDT6 is illustrated in Eqs. (9) to (11), while the obtained Pareto front on this function is given in Fig. 8. In the rest of the paper, this algorithm was used for optimization of the process.

$$f_1(x) = 1 - exp(-4x_1)\, sin^6(6\pi_1) \tag{9}$$

$$f_2(x) = g(x)[1 - (f_1(x)/g(x))^2] \;\; 0 \le x_i \le 1 \tag{10}$$

$$g(x) = 1 - 9[(\sum_{i=2}^{n} x_i)/(n-1)]^{0.25} i = 2,\ldots..n \tag{11}$$

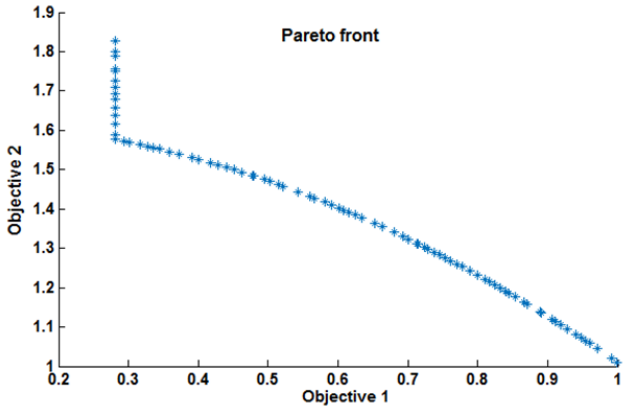

Fig. 8. NSGA-II Pareto front on the test function of ZDT6.

4.2.2. Optimization of the machining process

After developing the modified NSGA-II, the hybrid method of ANN-NSGA-II was implemented for simultaneous optimization of the process. For this purpose, the inverse of the Machining Time (one of the input parameters) was directly taken into account as one of the objective functions and the function implemented by the neural network for surface roughness was defined as another objective function. In fact, after each generation in optimization algorithm, the machining parameters are updated so that the surface roughness is reduced and Machining Time (MT) is simultaneously increased. This procedure is continued to obtain optimal conditions. The flowchart of the implemented strategy for optimization of the process and reach the optimal Pareto front is shown in Fig. 9. The optimal Pareto front is also given in Fig. 10.

It should be underlined that the aim of this strategy is to find the optimal tool life and machining conditions that cause a low surface roughness at the machined workpiece. After optimization, a number of 40 non-dominated solutions were obtained. All of these solutions are optimal solutions and any of them is not absolutely better than others. In fact, each solution is better than others in one objective function and they can be selected according to the costumers' requirement. In order to better analyse, the results of multi-objective optimization were summarized, classified and then reported in Table 3.

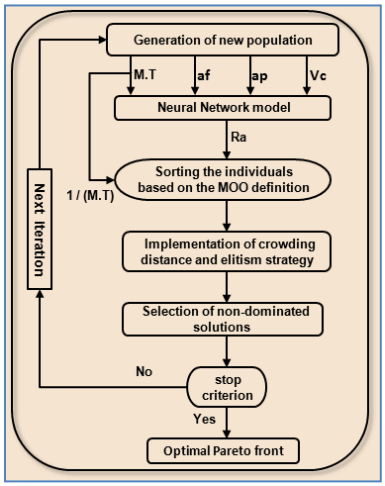

Fig. 9. Implemented strategy for multi-objective optimization.

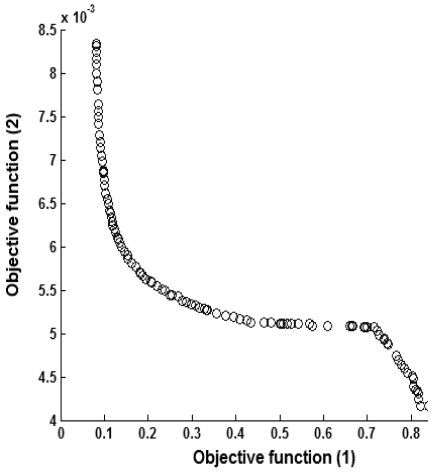

Fig. 10. Optimal Pareto front.

Table 3. The summarized results of the multi-objective optimization.

N	Machining parameters			Machining outputs range	
	ap **(mm)**	***Vc*** **(m/min)**	***af*** **(rev/min)**	**M.T. (s)**	***Ra*** **(*μm*)**
1	0.2	150	0.08	120 < M. T < 155	0.082 < *Ra* < 0.11
2	0.2	150	0.08	155 < M. T < 180	0.11 < *Ra* < 0.20
3	0.2	150	0.08	180 < M. T < 194	0.20 < *Ra* < 0.40

The results indicate that the machining time when reach a critical level plays important rule on the quality of the machined surfaced and determination of the optimal tool life is an essential task in the machining process. In order to obtain the optimal conditions, the depth of cut, cutting speed, feed rate should be maintained 0.2 (mm), 150 (m/min) and 0.08 (mm/rev), respectively. More in detail, when the depth of cut is increased, tool vibration is also increased and consequently, this event deteriorates the surface quality of the machined workpiece. As reported in the literature, cutting speed (*Vc*) and feed rate (*af*) has a negative or a positive effect on surface roughness in machining of Inconel 718 alloy [26, 27]. Since Built-Up-Edge (BUE) formation is machining of Inconel 718 is evident due to the inducing high mechanical and thermal loads during the process, depending on the investigated range of *Vc* and *af*, BUE formation in machining of Inconel 718 can be detrimental. Higher cutting speeds lead to the softening the material and BUE is jointed to the chip and not in the machined surface. Besides, increasing the *af* does

not provide enough time for BUE to be jointed in the machined surface and it will be far away from cutting zone by rapid chip formation. It was also found that the machining time less than 155 seconds leads to the minimal surface roughness (less than 0.11 μm). In addition, with increasing the machining time up to 180 seconds the surface roughness was still satisfactory (less than 0.2 μm) so that this process conditions can be used as the suitable alternative for grinding process. However, the surface roughness was significantly increased after 180 seconds. As explained in this section, there is a conflict between machining time and surface roughness and the critical machining time should be correctly selected based on to the engineers' requirement.

5. Conclusion

In this paper, an experimental investigation was carried out to evaluate the effect of tool wear and cutting parameters on surface roughness in turning process of Inconel 718 superalloy. The efficient intelligent techniques based on the *ANN* and MOO was employed to simultaneous optimization of tool life and surface roughness during the process.

- The elitism strategy was added to the NSGA-II and the algorithm was successfully examined on a testing function.
- It was found that increasing the machining time up to 180 seconds leads to the satisfactory surface roughness (less than 0.2 μm). After 180 seconds machining, worn tool geometry reached to the critical level that affected the surface quality of the machined workpiece.
- Results of multi-objective optimization indicated all of the optimal conditions were accessed at the depth of cut, cutting speed and feed rate 0.2 (mm), 150 (m/min) and 0.08 (mm/rev), respectively. Tool vibration and BUE formation generated by variation of machining parameters were recognized to be an effective factor that influences on surface quality.
- Finally, it can be said that implemented strategy in this paper provides an efficient approach to determine desirable tool life in machining processes. Based on this, the effect of tool wear is deserved to be taken into account on the other indications of surface integrity such as residual stress in future.

Nomenclatures

f_k	Is kth solution in the objective space
f_k^{max}	Maximum solution of the objective function k
f_k^{min}	Minimum solution of the objective function k
af	Feed rate
ap	Depth of cut
B_2	Matrix of output layer biases
B_h	Number of the hidden layer biases
B_o	Number of the output layer biases
F	Number of the inputs
$F(x)$	Objective functions of optimization in the objective space Z
I	Input matrix value of the neural network
K	Number of the objective function

L_{32}	Orthogonal array in Taguchi method
N	Number of optimization variables
N_h	Number of the neurons of the hidden layer
N_j	Number of allowable population
N_o	Number of the output layer neurons
p_1 *to* p_{17}	Optimization variables
P_t	Input variables in NSGA
P_{t+1}	Parent population in NSGA
Ra	Arithmetic average value of filtered roughness profile, μm
Vc	Cutting speed
W_1	Matrix for weights between input and hidden layer
W_2	Matrix for weights between hidden layer and output layer
X	Decision space
x_1 *to* x_n	Vector of input variables
Z	Objective space
Z_2	Output value of the neural network

Greek Symbols

μm	Micrometre

Abbreviations

ANN	Artificial Neural Network
BUE	Built-Up Edge
CBN	Cubic Boron Nitride
CD	Crowding Distance
GA	Genetic Algorithm
GONNS	Genetically Optimized Neural Network System
HRC	Hardness Rockwell
MT	Machining Time
MOO	Multi-Objective Optimization
MQL	Minimum Quantity Lubricant
MSE	Mean Square Error
NSGA	Non-Dominated Sorting Genetic Algorithm
TGRA	Taguchi Grey Relational Analysis

References

1. Jafarian, F.; Masoudi, S.; Soleimani, H.; and Umbrello, D. (2018). Experimental and numerical investigation of thermal loads in Inocnel 718 machining. *Materials and Manufacturing Processes*, 33(9), 1020-1029.
2. Jafarian, F.; Umbrello, D.; and Jabbaripour, B. (2016). Identification of new material model for machining simulation of Inconel 718 alloy and the effect of tool edge geometry on microstructure changes. *Simulation Modelling Practice and Theory*, 66, 273-284.
3. Hao, Z.; Gao, D.; Fan, Y.; and Han, R. (2011). New observations on tool wear mechanism in dry machining Inconel718. *International Journal of Machine Tools and Manufacture*, 51(12), 973-979.
4. Davim, J.P. (2008). *Machining*. Fundamental and recent advances. London: Springer-Verlag.

5. Davim, J.P. (2010). *Surface integrity in machining*. London: Springer-Verlag.
6. Khidhir, B.A.; and Mohamed, B. (2010). Study of cutting speed on surface roughness and chip formation when machining nickel-based alloy. *Journal of Mechanical Science and Technology*, 24(5), 1053-1059.
7. Jianxin, D.; Lili, L.; Jianhua, L.; Jinlong, Z.; and Xuefeng, Y. (2005). Failure mechanisms of TiB2 particle and SiC whisker reinforced Al_2O_3 ceramic cutting tools when machining nickel-based alloys. *International Journal of Machine Tools and Manufacture*, 45(12-13), 1393-1401.
8. Darwish, S.M. (2000). The impact of the tool material and the cutting parameters on surface roughness of Supermet 718 Nickel Superalloy. *Journal of Materials Processing Technology*, 97(1-3), 10-18.
9. Thakur, D.G.; Ramamoorthy, B.; and Vijayaraghavan, L. (2009). A study on the parameters in high-speed turning of Superalloy Inconel 718. *Journal of Materials and Manufacturing Processes*, 24(4), 497-503.
10. Altin, A.; Nalbant, M.; and Taskesen, A. (2008). The effects of cutting speed on tool wear and tool life when machining Inconel 718 with ceramic tools. *Materials and Design*, 28(9), 2518-2522.
11. Ezugwu, E.O.; Bonney, J.; Fadare, D.A.; and Sales, W.F. (2005). Machining of nickel-base, Inconel 718, alloy with ceramic tools under finishing conditions with various coolant supply pressures. *Journal of Materials Processing Technology*, 162-163, 609-614.
12. Kaynak, Y. (2014). Evaluation of machining performance in cryogenic machining of Inconel 718 and comparison with dry and MQL machining. *The International Journal of Advanced Manufacturing Technology*, 72(5-8), 919-933.
13. Yusup, N.; Zain, A.M.; and Hashim, S.Z.M. (2012). Evolutionary techniques in optimizing machining parameters: Review and recent applications (2007-2011). *Expert Systems with Applications*, 39(10), 9909-9927.
14. Ezugwu, E.O.; Fadare, D.A.; Bonney, J.; Da Silva, R.b.; and Sales, W.F. (2005). Modelling the correlation between cutting and process parameters in high-speed machining of Inconel 718 alloy using an artificial neural network. *International Journal of Machine Tools and Manufacture*, 45(12-13), 1375-1385.
15. Homami, R.M.; Tehrani, A.F.; Mirzadeh, H.; Movahedi, B.; and Azimifar, F. (2014). Optimization of turning process using artificial intelligence technology. *The International Journal of Advanced Manufacturing Technology*, 70(5-8), 1205-1217.
16. Jafarian, F.; Amirabadi, H.; and Fattahi, M. (2014). Improving surface integrity in finish machining of Inconel 718 alloy using intelligent systems. *The International Journal of Advanced Manufacturing Technology*, 71(5-8), 817-827.
17. Pawade, R.S.; and Joshi, S.S. (2011). Multi-objective optimization of surface roughnessand cutting forces in high-speed turning of Inconel 718 using Taguchi grey relational analysis (TGRA). *The International Journal of Advanced Manufacturing Technology*, 56(1-4), 47-62.

18. Zain, A.M.; Haron, H.; and Sharif, S. (2010). Prediction of surface roughness in the end milling machining using Artificial Neural Network. *Expert Systems with Applications*, 37(2), 1755-1768.
19. Lee, M.J.; Case, K.; and Marshall, R. (2016). Product lifecycle optimization of car climate controls using analytical hierarchical process (AHP) analysis and a multi-objective grouping genetic algorithm (MOGGA). *Journal of Engineering Science and Technology* (*JESTEC*), 11(1), 001-017.
20. Jafarian, F.; Taghipour, M.; and Amirabadi, H. (2013). Application of artificial neural network and optimization algorithms for optimizing surface roughness, tool life and cutting forces in turning operation. *Journal of Mechanical Science and Technology*, 27(5), 1469-1477.
21. Jafarian, F.; Amirabadi, H.; and Sadri, J. (2013). Integration of finite element simulation and intelligent methods for evaluation of thermo-mechanical loads during hard turning process. *Proceedings of the Institution of Mechanical Engineers, Part B: Journal of Engineering Manufacture*, 227(2), 235-248.
22. Kumar, G.S.; Padmanabhan, G.; and Sarma, B.D. (2016). Simultaneous optimization of hot and cold outlet air temperatures of vortex tube using grey relational analysis and Taguchi method. *Journal of Engineering Science and Technology* (*JESTEC*), 11(11), 1543-1553.
23. Radzali, S.A.; Masturah, M.; Baharin, B.S.; Rashidi, O.; and Rahman, R.A. (2016). Optimization of superficial fluid extraction of astaxanthin from penaeus monodon waste using ethanol-modified carbon dioxide. *Journal of Engineering Science and Technology* (*JESTEC*), 11(5), 722-736.
24. Jafarian, F.; Amirabadi, H.; Sadri, J.; and Banooie, H.R. (2014). Simultaneous optimizing residual stress and surface roughness in turning of Inconel 718 Superalloy. *Journal of Materials and Manufacturing Processes*, 29(3), 337-343.
25. Wang, L.; Wang, T.-g.; and Luo, Y. (2011). Improved non-dominated sorting genetic algorithm (NSGA)-II in multi-objective optimization studies of wind turbine blades. *Applied Mathematics and Mechanics*, 32(6), 739-748.
26. Ezugwu, E.O.; Fadare, D.A. Bonney, J.; Da Silva, R.B.; and Sales W.F. (2005). Modelling the correlation between cutting and process parameters in high-speed machining of Inconel 718 alloy using an artificial neural network. *International Journal of Machine Tools and Manufacture*, 45(12-13), 1375-1385.
27. Kumar, S.; Singh, D.; and Kalsi, N.S. (2017). Experimental investigations of surface roughness of Inconel 718 under different machining conditions. *Materials Today: Proceedings*, 4(2), 1179-1185.